

Fate of entanglement in open quantum spin liquid: Time evolution of its genuine multipartite negativity upon sudden coupling to a dissipative bosonic environment

Federico Garcia-Gaitan and Branislav K. Nikolić*

Department of Physics and Astronomy, University of Delaware, Newark, DE 19716, USA

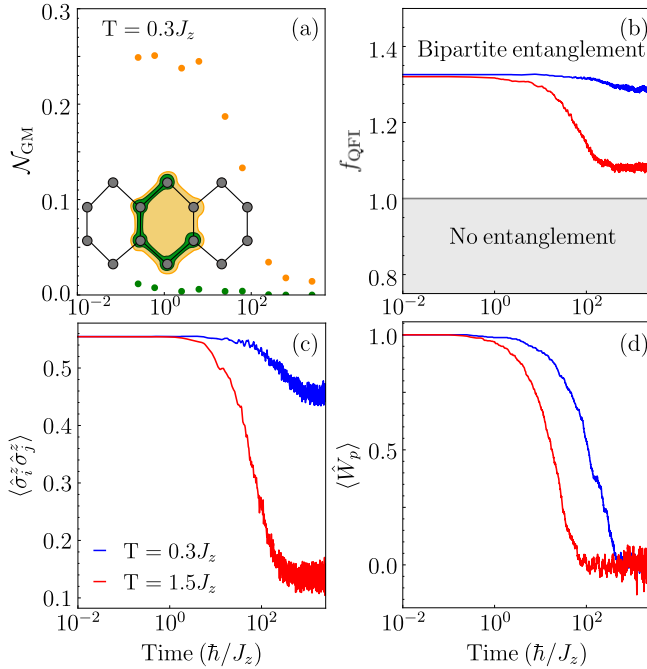
Topological properties of many-body entanglement in quantum spin liquids (QSLs), persisting at arbitrarily long distances, have been intensely explored over the past two decades, but mostly for QSLs viewed as *closed* quantum systems. However, in experiments and potential quantum computing applications, candidate materials for this exotic phase of quantum matter will always interact with a dissipative environment, such as the one generated by bosonic quasiparticles in solids at finite temperature. Here we investigate the *spatial distribution* of entanglement and its *stability* for the Kitaev model of QSL made *open* by sudden coupling to an infinite bosonic bath of Caldeira-Leggett type and time-evolved using the Lindblad quantum master equation in the Markovian regime (i.e., for weak coupling) or tensor network methods for open quantum systems in the non-Markovian regime (i.e., for strong coupling). From the time-evolved density matrix of QSL and its subregions, we extract genuine multipartite negativity (GMN), quantum Fisher information, spin-spin correlators, and expectation value (EV) of the Wilson loop operator. In particular, time-dependence of GMN offers the most penetrating insights: (i) in the Markovian regime, it remains non-zero in larger loopy subregions of QSL (as also discovered very recently for closed QSLs) up to temperatures comparable to Kitaev exchange interaction at which other quantities, such as EV of the Wilson loop operator, vanish; (ii) in the non-Markovian regime with pronounced memory effects, GMN remains non-zero up to even higher temperatures, while also acquiring non-zero value in smaller non-loopy subregions. The non-Markovian dynamics can also generate emergent interactions between spins, thereby opening avenues for tailoring properties of QSL via engineering of dissipation.

Introduction.—Quantum spin liquids (QSLs) [1, 2] are exotic phases of matter that, despite being composed of magnetic atoms, do not exhibit long-range magnetic ordering down to absolute zero temperature [3]. Nevertheless, they exhibit a wealth of emergent properties, such as topological ground-state degeneracy, long-range entanglement [2, 4–6], and fractionalization [3, 7–11] of its fundamental quantum spin degrees of freedom localized at crystalline lattice sites into quasiparticles like itinerant Majorana fermions, localized visons (i.e., vortex-like excitations of gauge field) and non-Abelian anyons (i.e., visons accompanied by a Majorana zero mode) and spinons. Due to fundamental interest, as well as potential applications of their long-range entanglement to realize scalable fault-tolerant quantum computation [5], materials hosting QSLs have been highly sought [1]. Despite diverse experimental probes applied to many candidate materials [12–15], a definitive proof for the existence of QSL phase remains elusive [15–17] (note that demonstration of QSL phase, using programmable quantum simulators composed ~ 200 Rydberg atoms, has been achieved [5]).

Since topologically ordered states appear to be liquid-like at short length scales, they cannot be characterized via traditional local order parameters and broken symmetry. Instead, topological entanglement entropy (TEE) [4, 18–21] has been intensely studied as a smoking gun of topological order in *pure* ground state |GS⟩ of QSL viewed as a *closed* quantum system. The TEE quantifies bipartite entanglement between a subregion of QSL and its complement, but it can fail to differentiate topological phases with distinct fractionalized excitations (for which TEE might be identical [22, 23])

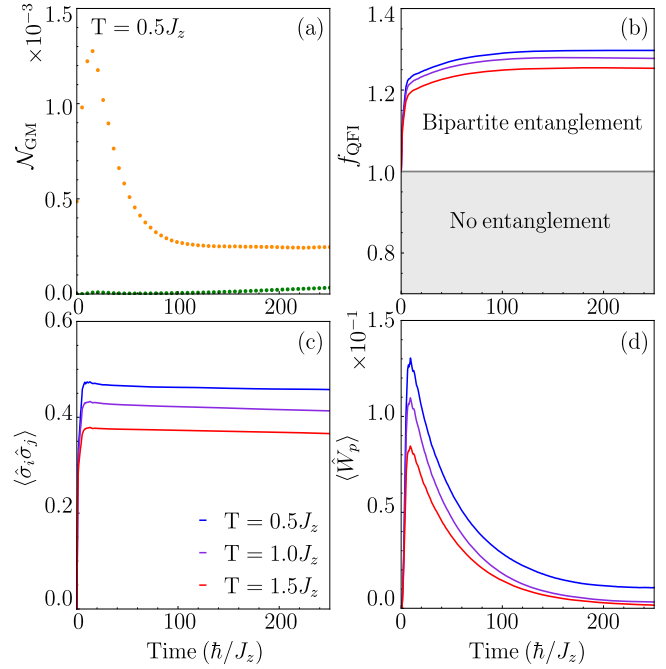
or produce spurious signals (such as non-zero TEE for topologically trivial GS [24]). A particularly interesting result on *spatial distribution* and *multipartite* nature of entanglement in closed QSLs has been obtained [25] very recently by analyzing the so-called genuine multipartite negativity (GMN) [26–28] for parties of m spins. This quantity employs the partial transpose operation used to detect entanglement of mixed quantum states via more familiar entanglement negativity [29–32], to which GMN reduces for $m = 2$ parties. For example, GMN shows that multipartite entanglement between spins is *absent* in the small non-loopy subregions, while it becomes nonzero when considering loop-shaped larger subregions. As GMN quantifies the collective form of entanglement between remote degrees of freedom, its very recently initiated [25] application to QSLs could lead to a new understanding of fractionalization and how gauge bosons can encode quantum information.

There has also been a growing recent interest in identifying proper entanglement measures for diagnosing topological phases of *mixed* quantum states, as generated by thermal fluctuations [30, 31] or decoherence (which can occur even when energy-exchange processes are suppressed [33, 34]) and dephasing [32, 35–38] as a major obstacle in present noisy intermediate-scale quantum devices. However, these approaches do not consider explicitly the structured [39–42] environment and thereby induced dissipation to which candidate materials are always exposed, typically due to bosonic quasiparticles in solids. Such an environment can lead to non-Gibbs mixed quantum states, even in the long time limit [39, 43], and it can also generate [44] new interactions between spins



that are not present in the original equilibrium Hamiltonian.

Although *open* quantum system approaches tailored for QSLs have emerged [10, 46–51], they typically assume simplified phenomenological models while focusing *exclusively* on the Markovian regime (i.e., when system-environment coupling is weak and environmental correlations are short compared to the timescale of the system evolution [39, 45]), as described by the Lindblad quantum master equation (QME) [45, 52, 53]. Since numerical time evolution of the density matrix via Lindblad QME becomes computationally expensive for many spins [54], most of such studies try to evade solving it altogether and instead focus on analyzing spectral properties of an effective non-Hermitian Hamiltonian (composed of the original QSL Hamiltonian plus Lindblad operators). This precludes understanding of the fate of long-range entanglement, as its quantification requires a time-evolved density matrix. Furthermore, the *non-Markovian* dynamics with pronounced memory effect [55, 56] of open QSLs, which is particularly relevant [57] in quantum computing applications, remains unaddressed. This might be related to the fact that evolution for an arbitrarily long time of large



number of degrees of freedom in any spatial dimension and for different types of infinite structured dissipative environments is even more challenging than Lindbladian dynamics and, in fact, not completely solved [39–42, 44] problem in open quantum system theory.

In this Letter, we investigate how robust the entanglement of QSL is via real-time evolution of its reduced density matrix $\hat{\rho}(t)$ in *both* Markovian and non-Markovian regimes. For this purpose, we utilize the universal Lindblad QME [45] in the former regime and tensor network (TN) methodologies [39–42] for open quantum systems or the reaction coordinate (RC) [58] + polaron [59, 60] method in the latter regime. The time evolution of QSL is initiated by coupling the Kitaev model [3], as the canonical example of QSL that is also exactly solvable in the closed case, to a bath of infinitely many bosonic modes described by the canonical Caldeira-Leggett model [61]. Using $\hat{\rho}(t)$, we compute the time dependence of: GMN; quantum Fisher information (QFI) [62, 63], which is also experimentally accessible [64, 65]; spin-spin correlators; and the Wilson loop operator [3, 66, 67]. Such comprehensive dissection of topological order and long-range entanglement of open QSL yields principals results summarized in Figs. 1–3. To facilitate their discussion, we first introduce key concepts and useful notation.

Models and methods.—The plain Kitaev QSL Hamiltonian describes localized quantum spins $S = 1/2$ that interact via highly anisotropic exchange interaction, as given by [3]

$$\hat{H}_{\text{QSL}} = - \sum_{\langle ij \rangle_x} J_x \hat{\sigma}_i^x \hat{\sigma}_j^x - \sum_{\langle ij \rangle_y} J_y \hat{\sigma}_i^y \hat{\sigma}_j^y - \sum_{\langle ij \rangle_z} J_z \hat{\sigma}_i^z \hat{\sigma}_j^z. \quad (1)$$

Here, $(\hat{\sigma}_i^x, \hat{\sigma}_i^y, \hat{\sigma}_i^z)$ is the vector of the Pauli matrices describing spin at site i of the honeycomb lattice; J_μ is the magnitude of the Ising-like exchange interaction; and $\langle ij \rangle_\mu$ denotes the nearest-neighbor (NN) bonds where $\mu = x, y, z$. This system is made open and dissipative by coupling it with one or many baths of infinitely many three-dimensional and isotropic bosonic modes [61], so that the Hamiltonian of the total system QSL+bath(s) becomes

$$\hat{H} = \hat{H}_{\text{QSL}} + \hat{H}_{\text{bath}} + \hat{V}. \quad (2)$$

We distinguish two cases: in the first one, denoted as “local coupling,” we couple each quantum spin to an independent bath so that

$$\hat{H}_{\text{bath}} = \sum_{ik} \omega_{ik} \hat{\mathbf{a}}_{ik}^\dagger \hat{\mathbf{a}}_{ik}, \quad \hat{V} = \sum_k g_k \sum_{i\mu} \hat{\sigma}_i^\mu (\hat{a}_{ik}^{\mu\dagger} + \hat{a}_{ik}^\mu); \quad (3)$$

in the second one, denoted as “global coupling,” only one bath is coupled to the total spin operators, so that

$$\hat{H}_{\text{bath}} = \sum_k \omega_k \hat{\mathbf{a}}_k^\dagger \hat{\mathbf{a}}_k, \quad \hat{V} = \sum_k g_k \sum_{i\mu} \hat{\sigma}_i^\mu (\hat{a}_k^{\mu\dagger} + \hat{a}_k^\mu). \quad (4)$$

Here bosonic operators $\hat{\mathbf{a}}_k = (\hat{a}_k^x, \hat{a}_k^y, \hat{a}_k^z)^T$ and $\hat{\mathbf{a}}_{ik} = (\hat{a}_{ik}^x, \hat{a}_{ik}^y, \hat{a}_{ik}^z)^T$ annihilate modes of frequency ω_k and ω_{ik} , respectively. The spectral content of bosonic baths is specified [61] by $J(\omega) = 2\pi \sum |g_k|^2 \delta(\omega - \omega_k)$. For our numerical calculations, we choose the so-called Ohmic [68] bath whose spectral function is $J(\omega) = \Gamma \omega \exp(-\omega^2/2\Lambda^2) / [1 - \exp(-\omega/T)]$, where T is the temperature (we set $k_B = 1$), Γ is the single parameter characterizing the system-bath coupling, and Λ sets the exponential cutoff for high frequencies [45]. Note that the hallmark of the Ohmic bath is $J(\omega) \propto \omega$ at low frequencies.

By assuming small g_k , a QME of the Lindblad type [52, 53] can be derived for the reduced density matrix $\hat{\rho}$ of QSL only after bosonic bath(s) are traced over. However, standard approximations used in such derivations fail for systems with closely spaced (i.e., quasidegenerate) energy levels, as is the typical case with quantum magnets [69, 70]. Thus, to obtain Lindblad QME for open QSL in the Markovian regime, we follow the procedure of Ref. [45], yielding the so-called universal Lindblad QME. This QME [45] operates with three Lindblad operators $\hat{L}_{i\mu}$ per bath, so assuming N such baths, we obtain the

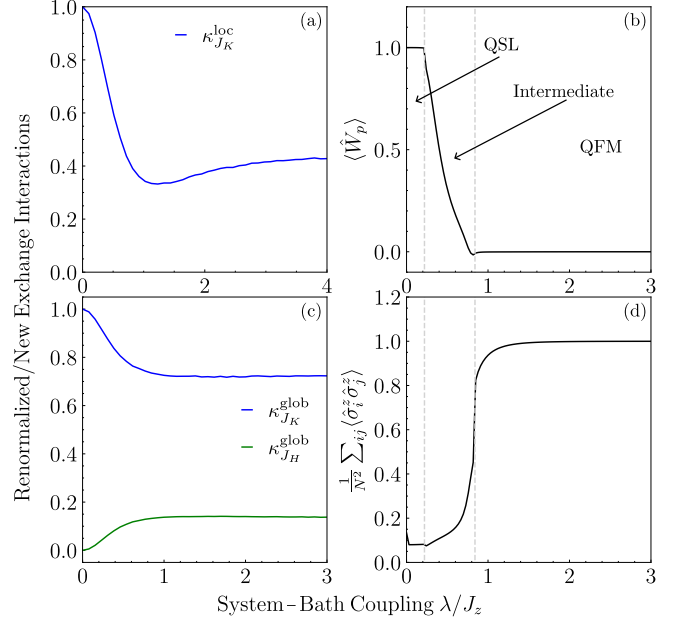


FIG. 3. Renormalized exchange interactions of Kitaev QSL Hamiltonian [Eq. (1)] for: (a) “local coupling” to many baths [Eq. (3)]; and (c) “global coupling” to a single bath [Eq. (4)]. (b) EV of Wilson loop operator for the case of “global coupling.” (d) Static FM structure factor for the system corresponding to panel (c). These results were obtained by diagonalizing the effective Hamiltonian [Eq. (A5)] produced by RC + polaron methodology, so they describe steady state in the long-time limit of *non-Markovian* dynamics generated by arbitrary strong coupling to a single global bath. The frequency of the RC was set to $\Omega = 8J_z$. Note that the limit $\lambda/J_z \rightarrow 0$ corresponds to the Markovian dynamics in Fig. 1.

following QME

$$d\hat{\rho}/dt = -i[\hat{H}_{\text{QSL}}, \hat{\rho}] + \sum_{i\mu}^N \left[\hat{L}_{i\mu} \hat{\rho} \hat{L}_{i\mu}^\dagger - \frac{1}{2} \{ \hat{L}_{i\mu}^\dagger \hat{L}_{i\mu}, \hat{\rho} \} \right], \quad (5)$$

where the Lamb-shift corrections to the Hamiltonian are neglected. We compute $\hat{L}_{i\mu}$ as a power series (where we use cutoff $N_L \leq 5$)

$$\hat{L}_{i\mu} = \sum_{n=0}^{N_L} c_n (\text{ad}_{\hat{H}_{\text{QSL}}})^n [\hat{A}_{i\mu}], \quad c_n = \frac{(-i)^n}{n!} \int_{-\infty}^{\infty} dt g(t) t^n, \quad (6)$$

thereby evading exact diagonalization of the full QSL Hamiltonian [45, 71]. Here $\text{ad}_{\hat{H}}[\hat{X}] = [\hat{H}, \hat{X}]$; $\hat{A}_{i\mu} = \hat{\sigma}_i^\mu$ in the “local coupling” case [Eq. (3)] or $\hat{A}_\mu = \sum_j \hat{\sigma}_j^\mu$ in the “global coupling” case [Eq. (4)]; and the jump correlator function is defined via the Fourier transform of the spectral function of the bath, $g(t) = \frac{1}{\sqrt{2\pi}} \int_{-\infty}^{\infty} d\omega \sqrt{J(\omega)} e^{-i\omega t}$. The universal Lindblad QME is solved using the quantum trajectories method [72], with up to ~ 1000 trajectories, as implemented in the QuTiP package [73, 74]. In these calculations we use $\Gamma = 0.001J_z$ and $\Lambda = 50T$.

For strong coupling of a system of a structured environment, generating non-perturbative effects and non-Markovian dynamics [56, 75], there is currently no universal solution for time-evolving the system akin to the Lindblad QME for the Markovian regime. Among a handful [39, 40, 42, 44, 76–78] of very recently developed methods that can handle many quantum spins as the system and arbitrary spectral function or temperature of their dissipative environment, we chose TN methodology [39–41] implemented as process tensor matrix product operator (PT-MPO). The PT-MPO combined time-evolving block decimation (TEBD), as available in open-source **OQuPy** package [40], allows us to perform real-time evolution of open QSL while also offering multitime two-spin correlators, which are not available when only the density matrix is known from time-evolution via non-Markovian QMEs [56, 75, 79, 80]. Note that for time-evolution of open QSL via **OQuPy** package [40] we are restricted to coupling the same local bosonic bath to a single component of spin at site i , thereby making it a particular case of the “local coupling” case. In PT-MPO+TEBD calculations, we use $\Lambda = 4J_z$ and stronger $\Gamma = 0.1J_z$. To set the system having only the NN interactions, we considered supersites composed of two physical spins so that the hexagonal ladder becomes effectively a chain. The PT-MPO+TEBD is then created with a maximum tolerance of 0.01 and the time evolution is performed keeping a maximum relative error of $\mathcal{O}(10^{-5})$ [40]. Since PT-MPO+TEBD calculations via **OQuPy** package [40] are challenging to start from an entangled initial state, we use $\hat{\rho}(t=0) = (\mathbf{I} \otimes \mathbf{I} \otimes \cdots \otimes \mathbf{I})/2^N$ for N spins, which is also a computationally favorable choice. Here the Kronecker product contains $N/2$ terms \mathbf{I} , where \mathbf{I} is the unit 4×4 matrix, so that $\mathbf{I}/4$ is the density matrix of two spins within the supersite. This choice does not affect conclusions in the long-time limit, as entanglement is quickly built dynamically [Figs. 2(a) and 2(b)] despite zero entanglement in $\hat{\rho}(t=0)$. Note that each supersite is coupled to an independent bath via the $\hat{\sigma}^z$ operator associated with one of the two spins within the supersite.

Finally, since TN methods can encounter an “entanglement barrier” [81–83], which prevent reaching truly long evolution times, to access long-time limit of non-Markovian dynamics we also employ the RC method [58] combined with polaron transformation [59]—this approach produces an effective Hamiltonian that can accurately [84] describe the steady-state of non-Markovian dynamics. The same strategy has been applied previously to classify possible magnetic orderings of steady-states in the case of dissipative quantum spin chains [60]. We explain this strategy for open QSL in the End Matter.

Results and discussion.—We consider the Kitaev QSL composed of $N = 14$ spins $S = 1/2$ located on the sites of three hexagons [see insert of Fig. 1(a) for illustration],

for which $J_z = J_x = J_y = 1$ sets the unit of energy. Its GMN vs. time is shown in Figs. 1(a) and 2(a) for the Markovian and non-Markovian regimes, respectively. Let us recall [25–27] that a finite GMN value indicates that for *all possible* bipartitions into subregions 1 and 2 of the total quantum system its density matrix remains entangled, $\hat{\rho} \neq \sum_n p_n \hat{\rho}_n^1 \otimes \hat{\rho}_n^2$. Thus, diagnostics of entanglement offered by GMN is more general than either the von Neumann and Renyi entropies [85], which apply only to pure quantum states; or logarithmic negativity routinely employed [29, 31, 32, 86] to detect entanglement in mixed quantum states but only by considering a single bipartition. Since evaluation of GMN is computationally highly expensive, it is currently restricted to 6 spins [25, 26]. This is why in Figs. 1(a) and 2(a) we compute GMN for a loopy subregion of 6 spins [such as those residing on all sites encompassed by the yellow hexagon in the inset of Fig. 1(a)]; as well as for a non-loopy subregion of 5 spins (such as those encompassed by the green bonds in the inset of these figures). Note that the same subregions were considered in Ref. [25] for closed Kitaev QSL, where the density matrix of subregions arises from $\hat{\rho}_{\text{subregion}} = \text{Tr}_{\text{other}} |\text{GS}\rangle \langle \text{GS}|$. In contrast, in our calculations for open Kitaev QSL $\hat{\rho}_{\text{subregion}}(t) = \text{Tr}_{\text{other}} \hat{\rho}(t)$. In the Markovian regime, non-loopy subregions can exhibit small non-zero GMN [green dots in Fig. 1(a)] because of the environment, but at longer times this vanishes, as is the case of closed Kitaev QSL [25]. The GMN of loopy subregions decays with time [orange dots in Fig. 1(a)], but it saturates at a finite value as long as temperature $T < 0.5J_z$.

In the non-Markovian regime, non-loopy subregions acquire non-zero GMN [green dots in Fig. 2(a)], increasing with time, which is quite *different* from closed Kitaev QSL [25]. The GMN of loopy subregions remains finite [orange dots in Fig. 2(a)] in the non-Markovian regime, up to temperature $T < 0.7J_z$. It is also worth comparing the time evolution of GMN in open QSL vs open quantum antiferromagnet (QAF), both of which are defined on the same honeycomb lattice. As shown in Fig. S1 of the Supplemental Material (SM) [87], GMN remains non-zero in both non-loopy (in contrast to zero value in QSL in Fig. 1(a) and Ref. [25]) and loopy subregions in the course of Markovian dynamics.

While entanglement entropy of pure states of cold atom simulators of quantum magnets has been directly measured [85], this is not possible in the case of solid-state magnetic materials. Instead, recent efforts have focused on extracting entanglement witnesses [62, 88], which are functionals of the density matrix not requiring its full tomography [89], both in [64, 90] and out [65, 91] of equilibrium. One such witness is QFI [64, 65, 90, 91], which motivates its computation in Figs. 1(b) and 2(b) using

the following expression [65, 86]

$$f_{\text{QFI}}(\mathbf{k}, t) = \frac{4}{N} \sum_{ij} e^{i\mathbf{k} \cdot (\mathbf{r}_i - \mathbf{r}_j)} \left\{ \text{Tr}[\hat{\rho}(t) \hat{\sigma}_i^z \hat{\sigma}_j^z] - \text{Tr}[\hat{\rho}(t) \hat{\sigma}_i^z] \text{Tr}[\hat{\rho}(t) \hat{\sigma}_j^z] \right\}, \quad (7)$$

where \mathbf{r}_i denotes the position of the site i of the lattice and k is the crystalline wavevector. Such time-dependent QFI [65, 86, 91] can witness n -partite entanglement by exhibiting $f_{\text{QFI}}(\mathbf{q}, t) \leq 4S^2n$. Thus, $f_{\text{QFI}}(\mathbf{k}, t) > 1$ indicates at least a bipartite entangled mixed state of the whole system. Figs. 1(b) and 2(b) show that the whole Kitaev QSL can remain bipartite entangled even at temperatures at which GMN of its subregions vanishes in Figs. 1(a) and 2(a).

As the next quantity, we compute the time evolution of the equal-time spin-spin correlator $\langle \hat{\sigma}_i^z(t) \hat{\sigma}_j^z(t) \rangle$ for two NN sites i and j in open Kitaev QSL. The same quantity has been amply studied in *closed* Kitaev QSL [7, 92, 93], where it is zero beyond NN sites $\langle \hat{\sigma}_i^\mu \hat{\sigma}_j^\nu \rangle \propto \delta^{\mu\nu} \delta_{\langle ij \rangle \mu}$, thereby signifying a lack of long-range magnetic ordering in QSL. We find the same feature in open QSL [Figs. 1(c) and 2(c)], on the proviso that “local coupling” [Eq. (3)] to many baths is used. If we use “global coupling” [Eq. (4)] to a single bath, such a bath introduces new correlations between spins in the non-Markovian regime [i.e., for sufficiently strong λ in Eq. (A1)], leading to the spin-spin correlator being *non-zero beyond* NN sites [Fig. 3(d)]. We also find that $\langle \hat{\sigma}_i^z(t) \hat{\sigma}_j^z(t) \rangle$ in the “local coupling” case decays with increasing time or temperature, with faster decay [compare Fig. 1(c) vs Fig. 2(c)] in the case of Markovian dynamics.

Figures 1(d) and 2(d) analyze the time dependence of EV of the Wilson loop operator, $\langle \hat{W}_p \rangle(t)$, in the Markovian and non-Markovian regimes, respectively. For Kitaev QSL, one often employs [94] $\hat{W}_p = \hat{\sigma}_1^z \hat{\sigma}_2^y \hat{\sigma}_3^x \hat{\sigma}_4^z \hat{\sigma}_5^y \hat{\sigma}_6^x$ for a loop of sites 1 to 6 forming the first hexagon in the inset of Fig. 1(a). We adopt the same Wilson loop operator, whose EV is obtained as $\langle \hat{W}_p \rangle(t) = \text{Tr}[\hat{\rho}(t) \hat{W}_p]$. This operator for a closed Kitaev QSL at zero temperature indicates ordering of fluxes as one of its fractionalized excitations within the model, and it has also been employed to study their disordering due to thermal fluctuations [94]. For open Kitaev QSL, we find that $\langle \hat{W}_p \rangle(t)$ decays with time in Figs. 1(d) and 2(d), with faster decay at higher temperature. Nevertheless, both GMN and QFI in Figs. 1 and 2 remain non-zero in the same long-time limit. Note that in the non-Markovian regime, $\langle \hat{W}_p \rangle(t) \neq 0$ [Fig. 2(d)] in the long-time limit for sufficiently low temperatures of the bosonic baths.

Finally, to handle a *single* global bosonic bath, we employ the RC + polaron method (see End Matter). This method also makes it possible to construct an effective Hamiltonian [87] whose low-energy eigenstates provide insight into the long-time limit properties of non-Markovian dynamics at arbitrary strength of QSL-bath

coupling. Unlike the “local coupling” case [Eq. (3)] studied in Figs. 1 and 2, in the “global coupling” case [Eq. (4)] we find new [green curve in Fig. 3(c)] bath-induced exchange interactions between spins or the renormalized old ones [blue curves in Figs. 3(a) and 3(c)]. These include all-to-all ferromagnetic Heisenberg exchange, $\kappa_{J_H}^{\text{glob}} \lambda^2 / \Omega$, interaction [Eq. (A5)], which grows with the system-bath coupling λ . Therefore, a phase transition from QSL to a quantum ferromagnet (QFM) could be expected [Fig. 3(d)]. In addition, the EV of the Wilson loop operator [Fig. 3(b)] shows that the QSL phase is stable in the weak coupling regime, as also observed in Markovian dynamics simulations [Fig. 1], before transitioning to an intermediate state [Fig. 3(b)]. Upon entering the strong coupling regime, $\lambda/J_z \gtrsim 0.8$, we find the emergence of the QFM phase [60]. Such a transition to the QFM phase for $\lambda/J_z \gtrsim 0.8$ is additionally confirmed by computing the static ferromagnetic structure factor [Fig. 3(d)].

Conclusions.—In contrast to amply studied bipartite entanglement [4, 18, 19], or very recently initiated multipartite entanglement [25], for *closed* QSLs, the fate of entanglement of QSLs made *open* by coupling them to a dissipative structured environment remains largely unexplored despite its relevance for experiments and quantum computing applications. Our direct real-time evolution of open Kitaev QSL, via Lindblad QME in the Markovian regime or TN methods in the non-Markovian regime, demonstrates how the *multipartite* entanglement quantified by GMN can be remarkable robust, persisting even at elevated temperatures of the environment at which signatures of fractionalized quasiparticles have vanished. This is akin to persistence of experimentally witnessed entanglement in other quantum magnets, such as in QAF, up to temperatures much higher than their magnetic ordering [64]. We also unravel how non-Markovian dynamics can induce novel effects, beyond the naïve expectation of environments simply diminishing the entanglement, such as non-zero GMN in non-loopy subregions or additional exchange interactions between spins. Our findings open pathways for engineering dissipation [95] and decoherence [36–38] to tailor properties of QSL candidate materials for topological quantum computing, which we relegate to future studies.

This work was supported by the U.S. National Science Foundation (NSF) under Grant No. DMR-2500816. The supercomputing time was provided by DARWIN (Delaware Advanced Research Workforce and Innovation Network), which is supported by NSF Grant No. MRI-1919839.

* bnikolic@udel.edu

[1] C. Broholm, R. J. Cava, S. A. Kivelson, D. G. Nocera, M. R. Norman, and T. Senthil, Quantum spin liquids,

Science **367**, eaay0668 (2020).

[2] L. Savary and L. Balents, Quantum spin liquids: a review, *Rep. Prog. Phys.* **80**, 016502 (2017).

[3] A. Kitaev, Anyons in an exactly solved model and beyond, *Ann. Phys.* **321**, 2 (2006).

[4] T. Grover, Y. Zhang, and A. Vishwanath, Entanglement entropy as a portal to the physics of quantum spin liquids, *New J. Phys.* **15**, 025002 (2013).

[5] G. Semeghini, H. Levine, A. Keesling, S. Ebadi, T. T. Wang, D. Bluvstein, R. Verresen, H. Pichler, M. Kalinowski, R. Samajdar, *et al.*, Probing topological spin liquids on a programmable quantum simulator, *Science* **374**, 1242 (2021).

[6] J. Knolle and R. Moessner, A field guide to spin liquids, *Annu. Rev. Condens. Matter Phys.* **10**, 451 (2019).

[7] J. Knolle, D. L. Kovrizhin, J. T. Chalker, and R. Moessner, Dynamics of a two-dimensional quantum spin liquid: Signatures of emergent Majorana fermions and fluxes, *Phys. Rev. Lett.* **112**, 207203 (2014).

[8] S.-H. Do, S.-Y. Park, J. Yoshitake, J. Nasu, Y. Motome, Y. Kwon, D. T. Adroja, D. J. Voneshen, K. Kim, T.-H. Jang, *et al.*, Majorana fermions in the Kitaev quantum spin system α -RuCl₃, *Nat. Phys.* **13**, 1079 (2017).

[9] J. Nasu, Majorana quasiparticles emergent in Kitaev spin liquid, *Prog. Theor. Exp. Phys.* **2024**, 08C104 (2023).

[10] C. Harada, A. Ono, and J. Nasu, Real-time control of non-Abelian anyons in Kitaev spin liquid under energy dissipation, *Phys. Rev. B* **110**, 214426 (2024).

[11] W. Zhu, S.-s. Gong, and D. N. Sheng, Identifying spinon excitations from dynamic structure factor of spin-1/2 Heisenberg antiferromagnet on the Kagome lattice, *PNAS* **116**, 5437 (2019).

[12] A. Banerjee, C. Bridges, J.-Q. Yan, A. Aczel, L. Li, M. Stone, G. Granroth, M. Lumsden, Y. Yiu, J. Knolle, *et al.*, Proximate Kitaev quantum spin liquid behaviour in a honeycomb magnet, *Nat. Mater.* **15**, 733 (2016).

[13] A. Banerjee, J. Yan, J. Knolle, C. Bridges, M. Stone, M. Lumsden, D. Mandrus, D. Tennant, R. Moessner, and S. Nagler, Neutron scattering in the proximate quantum spin liquid α -RuCl₃, *Science* **356**, 1055 (2017).

[14] C. Balz, P. Lampen-Kelley, A. Banerjee, J. Yan, Z. Lu, X. Hu, S. M. Yadav, Y. Takano, Y. Liu, D. A. Tennant, *et al.*, Finite field regime for a quantum spin liquid in α -RuCl₃, *Phys. Rev. B* **100**, 060405 (2019).

[15] Y. Kasahara, S. Suetsugu, T. Asaba, S. Kasahara, T. Shibauchi, N. Kurita, H. Tanaka, and Y. Matsuda, Quantized and unquantized thermal Hall conductance of the Kitaev spin liquid candidate α -RuCl₃, *Phys. Rev. B* **106**, L060410 (2022).

[16] S. M. Winter, K. Riedl, P. A. Maksimov, A. L. Chernyshev, A. Honecker, and R. Valentí, Breakdown of magnons in a strongly spin-orbital coupled magnet, *Nat. Commun.* **8**, 1152 (2017).

[17] P. A. Maksimov and A. L. Chernyshev, Rethinking α -RuCl₃, *Phys. Rev. Res.* **2**, 033011 (2020).

[18] A. Kitaev and J. Preskill, Topological entanglement entropy, *Phys. Rev. Lett.* **96**, 110404 (2006).

[19] M. Levin and X.-G. Wen, Detecting topological order in a ground state wave function, *Phys. Rev. Lett.* **96**, 110405 (2006).

[20] I. H. Kim, M. Levin, T.-C. Lin, D. Ranard, and B. Shi, Universal lower bound on topological entanglement entropy, *Phys. Rev. Lett.* **131**, 166601 (2023).

[21] M. Levin, Physical proof of the topological entanglement entropy inequality, *Phys. Rev. B* **110**, 165154 (2024).

[22] J. C. Bridgeman, S. T. Flammia, and D. Poulin, Detecting topological order with ribbon operators, *Phys. Rev. B* **94**, 205123 (2016).

[23] S. T. Flammia, A. Hamma, T. L. Hughes, and X.-G. Wen, Topological entanglement Rényi entropy and reduced density matrix structure, *Phys. Rev. Lett.* **103**, 261601 (2009).

[24] L. Zou and J. Haah, Spurious long-range entanglement and replica correlation length, *Phys. Rev. B* **94**, 075151 (2016).

[25] L. Lyu, D. Chandorkar, S. Kapoor, S. Takei, E. S. Sørensen, and W. Witczak-Krempa, Multiparty entanglement loops in quantum spin liquids, *arXiv:2505.18124* (2025).

[26] B. Jungnitsch, T. Moroder, and O. Gühne, Taming multiparticle entanglement, *Phys. Rev. Lett.* **106**, 190502 (2011).

[27] M. Hofmann, T. Moroder, and O. Gühne, Analytical characterization of the genuine multiparticle negativity, *J. Phys. A: Math. Theor.* **47**, 155301 (2014).

[28] M. Song, T.-T. Wang, L. Lyu, W. Witczak-Krempa, and Z. Y. Meng, Entanglement architecture of beyond-Landau quantum criticality, *arXiv:2509.09983* (2025).

[29] A. Peres, Separability criterion for density matrices, *Phys. Rev. Lett.* **77**, 1413 (1996).

[30] T.-C. Lu, T. H. Hsieh, and T. Grover, Detecting topological order at finite temperature using entanglement negativity, *Phys. Rev. Lett.* **125**, 116801 (2020).

[31] T.-C. Lu and S. Vijay, Characterizing long-range entanglement in a mixed state through an emergent order on the entangling surface, *Phys. Rev. Res.* **5**, 033031 (2023).

[32] R. Fan, Y. Bao, E. Altman, and A. Vishwanath, Diagnostics of mixed-state topological order and breakdown of quantum memory, *PRX Quantum* **5**, 020343 (2024).

[33] E. Joos, H. D. Zeh, C. Kiefer, D. J. W. Giulini, J. Kupsch, and I.-O. Stamatescu, *Decoherence and the Appearance of a Classical World in Quantum Theory* (Springer, Cham, 2003).

[34] M. Merkli, I. M. Sigal, and G. P. Berman, Decoherence and thermalization, *Phys. Rev. Lett.* **98**, 130401 (2007).

[35] J. Y. Lee, C.-M. Jian, and C. Xu, Quantum criticality under decoherence or weak measurement, *PRX Quantum* **4**, 030317 (2023).

[36] T. D. Ellison and M. Cheng, Toward a classification of mixed-state topological orders in two dimensions, *PRX Quantum* **6**, 010315 (2025).

[37] R. Sohal and A. Prem, Noisy approach to intrinsically mixed-state topological order, *PRX Quantum* **6**, 010313 (2025).

[38] Z. Wang, Z. Wu, and Z. Wang, Intrinsic mixed-state topological order, *PRX Quantum* **6**, 010314 (2025).

[39] G. E. Fux, D. Kilda, B. W. Lovett, and J. Keeling, Tensor network simulation of chains of non-Markovian open quantum systems, *Phys. Rev. Res.* **5**, 033078 (2023).

[40] G. E. Fux, P. Fowler-Wright, J. Beckles, E. P. Butler, P. R. Eastham, D. Gribben, J. Keeling, D. Kilda, P. Kirton, E. D. C. Lawrence, *et al.*, OQuPy: A Python package to efficiently simulate non-Markovian open quantum systems with process tensors, *J. Chem. Phys.* **161**, 124108 (2024).

[41] M. Cygorek, J. Keeling, B. W. Lovett, and E. M. Gauger, Sublinear scaling in non-Markovian open quantum systems simulations, *Phys. Rev. X* **14**, 011010 (2024).

[42] M. Cygorek and E. M. Gauger, ACE: a general-purpose non-Markovian open quantum systems simulation toolkit based on process tensors, *J. Chem. Phys.* **161**, 074111 (2024).

[43] F. Nathan and M. S. Rudner, Quantifying the accuracy of steady states obtained from the universal Lindblad equation, *Phys. Rev. B* **109**, 205140 (2024).

[44] F. Reyes-Osorio, F. Garcia-Gaitan, D. J. Strachan, P. Plechac, S. R. Clark, and B. K. Nikolić, Schwinger-keldysh nonperturbative field theory of open quantum systems beyond the Markovian regime: Application to spin-boson and spin-chain-boson models, [arXiv:2405.00765](https://arxiv.org/abs/2405.00765) (2025).

[45] F. Nathan and M. S. Rudner, Universal Lindblad equation for open quantum systems, *Phys. Rev. B* **102**, 115109 (2020).

[46] K. Yang, S. C. Morampudi, and E. J. Bergholtz, Exceptional spin liquids from couplings to the environment, *Phys. Rev. Lett.* **126**, 077201 (2021).

[47] K. Yang, D. Varjas, E. J. Bergholtz, S. Morampudi, and F. Wilczek, Exceptional dynamics of interacting spin liquids, *Phys. Rev. Res.* **4**, L042025 (2022).

[48] A. Kulkarni, T. Numasawa, and S. Ryu, Lindbladian dynamics of the Sachdev-Ye-Kitaev model, *Phys. Rev. B* **106**, 075138 (2022).

[49] H. Shackleton and M. S. Scheurer, Exactly solvable dissipative spin liquid, *Phys. Rev. B* **109**, 085115 (2024).

[50] K. Hwang, Mixed-state quantum spin liquids and dynamical anyon condensations in Kitaev Lindbladians, *Quantum* **8**, 1412 (2024).

[51] A. Coser and D. Pérez-García, Classification of phases for mixed states via fast dissipative evolution, *Quantum* **3**, 174 (2019).

[52] G. Lindblad, On the generators of quantum dynamical semigroups, *Commun. Math. Phys.* **48**, 119 (1976).

[53] D. Manzano, A short introduction to the Lindblad master equation, *AIP Adv.* **10**, 025106 (2020).

[54] A. Pocklington and A. A. Clerk, Efficient simulation of nontrivial dissipative spin chains via stochastic unraveling, *PRX Quantum* **6**, 030349 (2025).

[55] H.-P. Breuer, E.-M. Laine, J. Piilo, and B. Vacchini, Colloquium: Non-Markovian dynamics in open quantum systems, *Rev. Mod. Phys.* **88**, 021002 (2016).

[56] I. de Vega and D. Alonso, Dynamics of non-Markovian open quantum systems, *Rev. Mod. Phys.* **89**, 015001 (2017).

[57] B. Gulácsi and G. Burkard, Signatures of non-Markovianity of a superconducting qubit, *Phys. Rev. B* **107**, 174511 (2023).

[58] G. Schaller, *Open Quantum Systems Far from Equilibrium* (Springer, Cham, 2014).

[59] N. Anto-Sztrikacs, B. Min, M. Brenes, and D. Segal, Effective Hamiltonian theory: An approximation to the equilibrium state of open quantum systems, *Phys. Rev. B* **108**, 115437 (2023).

[60] B. Min, N. Anto-Sztrikacs, M. Brenes, and D. Segal, Bath-engineering magnetic order in quantum spin chains: An analytic mapping approach, *Phys. Rev. Lett.* **132**, 266701 (2024).

[61] A. J. Leggett, S. Chakravarty, A. T. Dorsey, M. P. A. Fisher, A. Garg, and W. Zwerger, Dynamics of the dissipative two-state system, *Rev. Mod. Phys.* **59**, 1 (1987).

[62] O. Gühne and G. Tóth, Entanglement detection, *Phys. Rep.* **474**, 1 (2009).

[63] G. D. Chiara and A. Sanpera, Genuine quantum correlations in quantum many-body systems: a review of recent progress, *Rep. Prog. Phys.* **81**, 074002 (2018).

[64] A. Scheie, P. Laurell, A. M. Samarakoon, B. Lake, S. E. Nagler, G. E. Granroth, S. Okamoto, G. Alvarez, and D. A. Tennant, Witnessing entanglement in quantum magnets using neutron scattering, *Phys. Rev. B* **103**, 224434 (2021).

[65] J. Hales, U. Bajpai, T. Liu, D. R. Baykusheva, M. Li, M. Mitrano, and Y. Wang, Witnessing light-driven entanglement using time-resolved resonant inelastic X-ray scattering, *Nat. Commun.* **14**, 3512 (2023).

[66] K. G. Wilson, Confinement of quarks, *Phys. Rev. D* **10**, 2445 (1974).

[67] M. B. Hastings and X.-G. Wen, Quasiadiabatic continuation of quantum states: The stability of topological ground-state degeneracy and emergent gauge invariance, *Phys. Rev. B* **72**, 045141 (2005).

[68] J. Anders, C. Sait, and S. Horsley, Quantum Brownian motion for magnets, *New J. Phys.* **24**, 033020 (2022).

[69] F. Garcia-Gaitan and B. K. Nikolić, Fate of entanglement in magnetism under Lindbladian or non-Markovian dynamics and conditions for their transition to Landau-Lifshitz-Gilbert classical dynamics, *Phys. Rev. B* **109**, L180408 (2024).

[70] N. Szpak, G. Schaller, R. Schützhold, and J. König, Relaxation to persistent currents in a Hubbard trimer coupled to fermionic baths, *Phys. Rev. B* **110**, 115131 (2024).

[71] A. Schnell, Global becomes local: Efficient many-body dynamics for global master equations, *Phys. Rev. Lett.* **134**, 250401 (2025).

[72] A. Daley, Quantum trajectories and open many-body quantum systems, *Adv. Phys.* **63**, 77 (2014).

[73] J. Johansson, P. Nation, and F. Nori, QuTiP 2: A Python framework for the dynamics of open quantum systems, *Comput. Phys. Commun.* **184**, 1234 (2013).

[74] N. Lambert, E. Giguère, P. Menczel, B. Li, P. Hopf, G. Suárez, M. Gali, J. Lishman, R. Gadhvi, R. Agarwal, *et al.*, QuTiP 5: The quantum toolbox in python, [arXiv:2412.04705](https://arxiv.org/abs/2412.04705) (2024).

[75] H.-P. Breuer and F. Petruccione, *The Theory of Open Quantum Systems* (Oxford University, Oxford, 2007).

[76] Y. Sun, G. Wang, and Z. Cai, Simulation of spin chains with off-diagonal coupling using the inchworm method, *J. Chem. Theory Comput.* **20**, 9321 (2024).

[77] M. Xu, J. T. Stockburger, and J. Ankerhold, Environment-mediated long-ranged correlations in many-body system, *J. Chem. Phys.* **161**, 124105 (2024).

[78] L. P. Lindoy, D. Rodrigo-Albert, Y. Rath, and I. Rungger, pyTTN: an open source toolbox for open and closed system quantum dynamics simulations using tree tensor networks, [arXiv:2503.15460](https://arxiv.org/abs/2503.15460) (2025).

[79] Y. Tanimura and R. Kubo, Time evolution of a quantum system in contact with a nearly Gaussian-Markoffian noise bath, *J. Phys. Soc. Jpn.* **58**, 101 (1989).

[80] M. Xu and J. Ankerhold, About the performance of perturbative treatments of the spin-boson dynamics within the hierarchical equations of motion approach, *Eur. Phys. J. Spec. Top.* **232**, 3209–3217 (2023).

[81] A. Lerose, M. Sonner, and D. A. Abanin, Overcoming the entanglement barrier in quantum many-body dynamics via space-time duality, *Phys. Rev. B* **107**, L060305 (2023).

[82] M. M. Rams and M. Zwolak, Breaking the entanglement

barrier: Tensor network simulation of quantum transport, *Phys. Rev. Lett.* **124**, 137701 (2020).

[83] A. Foligno, T. Zhou, and B. Bertini, Temporal entanglement in chaotic quantum circuits, *Phys. Rev. X* **13**, 041008 (2023).

[84] M. Brenes, B. Min, N. Anto-Sztrikacs, N. Bar-Gill, and D. Segal, Bath-induced interactions and transient dynamics in open quantum systems at strong coupling: Effective Hamiltonian approach, *J. Chem. Phys.* **160**, 244106 (2024).

[85] T. Brydges, A. Elben, P. Jurcevic, B. Vermersch, C. Maier, B. Lanyon, P. Zoller, R. Blatt, and C. Roos, Probing Rényi entanglement entropy via randomized measurements, *Science* **364**, 260 (2019).

[86] A. Suresh, R. D. Soares, P. Mondal, J. P. S. Pires, J. M. V. P. Lopes, A. Ferreira, A. E. Feiguin, P. Plecháč, and B. K. Nikolić, Electron-mediated entanglement of two distant macroscopic ferromagnets within a nonequilibrium spintronic device, *Phys. Rev. A* **109**, 022414 (2024).

[87] See Supplemental Material at <https://wiki.physics.udel.edu/qttg/Publications> for an additional figure showing the same information as in Figs 1 and 2, but for open QAF defined on the same honeycomb lattice as Kitaev QSL, as well as additional details in derivation of RC + polaron methodology.

[88] N. Friis, G. Vitagliano, M. Malik, and M. Huber, Entanglement certification from theory to experiment, *Nat. Rev. Phys.* **1**, 72 (2018).

[89] A. G. White, D. F. V. James, P. H. Eberhard, and P. G. Kwiat, Nonmaximally entangled states: Production, characterization, and utilization, *Phys. Rev. Lett.* **83**, 3103 (1999).

[90] P. Laurell, A. Scheie, E. Dagotto, and D. Tennant, Witnessing entanglement and quantum correlations in condensed matter: A review, *Adv. Quantum Technol.* **8**, 2400196 (2024).

[91] T. Ren, Y. Shen, S. F. R. TenHuisen, J. Sears, W. He, M. H. Upton, D. Casa, P. Becker, M. Mitrano, M. P. M. Dean, *et al.*, Witnessing quantum entanglement using resonant inelastic x-ray scattering, [arXiv:2404.05850](https://arxiv.org/abs/2404.05850) (2024).

[92] G. Baskaran, S. Mandal, and R. Shankar, Exact results for spin dynamics and fractionalization in the Kitaev model, *Phys. Rev. Lett.* **98**, 247201 (2007).

[93] H. Takegami and T. Morinari, Static and dynamical spin correlations in the Kitaev model at finite temperatures via Green's function equation of motion, *Phys. Rev. B* **111**, 054413 (2025).

[94] J. Nasu, M. Udagawa, and Y. Motome, Thermal fractionalization of quantum spins in a Kitaev model: Temperature-linear specific heat and coherent transport of Majorana fermions, *Phys. Rev. B* **92**, 115122 (2015).

[95] P. M. Harrington, E. J. Mueller, and K. W. Murch, Engineered dissipation for quantum information science, *Nat. Rev. Phys.* **4**, 660 (2022).

[96] J. Garwola and D. Segal, Open quantum systems with noncommuting coupling operators: An analytic approach, *Phys. Rev. B* **110**, 174304 (2024).

End Matter

RC + polaron methodology.—The RC method [58], which is based on the Bogoliubov transformation, introduces a new RC bosonic mode per each bath. They are created (annihilated) by an operator $\hat{b}_i^\dagger(\hat{b}_i)$, which is strongly coupled to the system but weakly coupled to the remaining modes of the bath. This transforms the Hamiltonian in Eq. (2) into

$$\hat{H}_{\text{RC}} = \hat{H}_{\text{QSL}} + \lambda \sum_i \hat{A}_{i\mu} (\hat{b}_i^\mu + \hat{b}_i^{\mu\dagger}) + \Omega \sum_i \hat{b}_i^\dagger \hat{b}_i + \hat{H}_{\text{RC-B}} + \hat{H}_{\text{bath}}, \quad (\text{A1})$$

where λ is the strength of the coupling between the RC mode and the system; Ω is the frequency of the RC mode; $\hat{H}_{\text{RC-B}} = \sum_i \sum_{k>1,\mu} \tilde{g}_k (\hat{b}_i^\mu + \hat{b}_i^{\mu\dagger})(\hat{c}_{ik}^\mu + \hat{c}_{ik}^{\mu\dagger})$ describes the coupling between the RC mode and the original bosonic bath; and $\hat{H}_{\text{bath}} = \sum_{i,k>1} \tilde{\omega}_k \hat{c}_{ik}^\dagger \hat{c}_{ik}$ is the Hamiltonian of residual bosonic modes. Here bosonic operators $\hat{c}_{ik} = (\hat{c}_{ik}^x, \hat{c}_{ik}^y, \hat{c}_{ik}^z)^T$, obtained by the Bogoliubov transformation of the original operators in Eq. (2), have frequency $\tilde{\omega}_k$. The second step of the RC + polaron methodology involves a polaron transformation [59, 60] per bath, incorporating the RC-system interaction strength directly into the system Hamiltonian. This transforms Hamiltonian in Eq. (A1) into

$$\hat{H}_{\text{RC+P}} = \prod_{i\mu} \hat{U}_P^{i\mu} \hat{H}_{\text{RC}} \hat{U}_P^{i\mu\dagger}, \quad (\text{A2})$$

where $\hat{U}_P^i = \prod_\mu \exp(\lambda/\Omega(\hat{b}_i^{\mu\dagger} - \hat{b}_i^\mu) \hat{A}_{i\mu})$ is the polaron transformation associated with the i -th bath. The final step projects the Hamiltonian onto the GS of each RC, which is an approximation valid in the low-temperature limit [59]. The resulting effective Hamiltonian is then given by

$$\hat{H}_{\text{eff}} = \text{Tr}_{\text{RC}}(\hat{\Pi}_0 \hat{H}_{\text{RC+P}} \hat{\Pi}_0), \quad (\text{A3})$$

where $\hat{\Pi}_0$ is the projection operator onto the product of GSs of each RC variable. Note that special care has to be taken in the case where the set of coupling operators $\{\hat{A}_{i\mu}\}$ do not commute [96], as is our case.

Application of Eq. (A3) to open Kitaev QSL [Eq. (2)] yields, for the “local coupling” case [Eq. (3)], the following effective Hamiltonian

$$\hat{H}_{\text{eff}}^{\text{loc}} = -\kappa_{J_K}^{\text{loc}}(\lambda/\Omega) \left[\sum_{\langle ij \rangle_x} J_x \hat{\sigma}_i^x \hat{\sigma}_j^x + \sum_{\langle ij \rangle_y} J_y \hat{\sigma}_i^y \hat{\sigma}_j^y + \sum_{\langle ij \rangle_z} J_z \hat{\sigma}_i^z \hat{\sigma}_j^z \right]. \quad (\text{A4})$$

We see that this Hamiltonian still has the Kitaev form in Eq. (1), but its exchange interactions are renormalized by prefactor $\kappa_{J_K}(\lambda/\Omega)$ whose dependence on QSL-bath coupling is plotted in Fig. 3(a). Further technical details of its derivation are provided in the SM [87]. Notably, as we couple each spin to three independent baths via non-commuting operators, the strength of the Kitaev ex-

change interaction does not decay to zero but instead stabilizes at a finite value [Fig. 3(a)].

In the “global coupling” case [Eq. (4)], an additional ferromagnetic Heisenberg exchange interaction term between spins on NN sites, as well as *all-to-all* ferromagnetic Heisenberg exchange, emerge due to the bath:

$$\hat{H}_{\text{eff}}^{\text{glob}} = - \sum_{\langle ij \rangle_\mu} J_\mu \kappa_{J_K}^{\text{glob}}(\lambda/\Omega) \hat{\sigma}_i^\mu \hat{\sigma}_j^\mu - \sum_{\langle ij \rangle} \sum_\mu J_\mu \kappa_{J_H}^{\text{glob}}(\lambda/\Omega) \hat{\sigma}_i \cdot \hat{\sigma}_j - \sum_{ij\mu} \frac{\lambda^2}{\Omega} \left(\kappa_{J_K}^{\text{glob}}(\lambda/\Omega) \hat{\sigma}_i^\mu \hat{\sigma}_j^\mu + \kappa_{J_H}^{\text{glob}}(\lambda/\Omega) \hat{\sigma}_i \cdot \hat{\sigma}_j \right). \quad (\text{A5})$$

Here $\kappa_{J_K}^{\text{glob}}(\lambda/\Omega)$ and $\kappa_{J_H}^{\text{glob}}(\lambda/\Omega)$ are the prefactors renormalizing Kitaev and Heisenberg exchange interactions,

respectively. They are plotted in Fig. 3(b) as a function of QSL-bath coupling.